Proceedings of the 9th IEEE International
Conference on Nano/Micro Engineered and Molecular Systems
April 13-16, 2014, Hawaii, USA

Position Determination of A Ball Grid Array by Automated Optical Inspection Method

Yi-Chuan Lin
National Changhua University of Education
Changhua, Taiwan
m0151022@mail.ncue.edu.tw

Kerwin Wang
National Changhua University of Education
Changhua, Taiwan
kerwin@cc.ncue.edu.tw

***Abstract* — This paper introduces a novel automated optical inspection (AOI) method to measure the positions and diameters of micro-solder balls of a ball grid array (BGA). The method is focused on the refinement of optical configuration, image acquisition platform design to improve the time efficiency of AOI. We use a white LED ring as a light source. It is combined with the platform. The system can perform multiple image processing and object detection steps to locate the center of each ball. This paper also presents two methods to estimate the diameters of the balls. A dummy BGA, consists of misaligned solder balls, are assembled to a conductive substrate to evaluate the platform. Test result shows that the platform is capable of performing continuous image acquisition of a 15fps, 640 × 480, 8-bite grayscale video.**

Keywords — automated optical inspection; image acquisition; ball grid array.

I. INTRODUCTION

BGA has been widely used in the microelectronics packaging processes recently [1]. BGA consists of an array of micro-solder balls with a diameter of 50~800μm. It offers densely packed conductive tunnel and heat dissipation path between two assembled chips to ensure the quality of the interconnections between two chips. It is critical to maintain a good consistency of the quality and reliability of the micro-assembled solder-balls [2].

There are many BGA inspection methods have been proposed. Visual inspection, using optical microscopy, is one of the most traditional methods. However, this method need well trained, highly skilled and experienced operators to perform well and consistent inspection quality. The inspection criteria and reliability may be different from person to person.

Roha et al. [3] introduced X-ray system to detect the flaws at solder joints, which is difficult to locate by visual or a normal x-ray imaging method. Yen et al. [4] designed a cost-effective 3D measurement system for BGA screening. The system uses an LCD-based phase measuring technique to gauge the 3D profile of a complete array of BGA. The process time is less than 2 sec. Kim and Rhee [5] developed a laser scanning and vision system for evaluating the height, co-planarity and lead pitch of BGA. Wang and his group members [6, 7] introduced a projective shadowing optic setup. This concise and elegant system uses white light emitting diodes as a light source to obtain the edge and shadow images of the balls for height calculation.

To meet the time-efficient demands of the package industry, in this paper, we further simplify the system optics design. The system consists of a ring light illuminator, a macro-lens, and a CCD image capturing system. The optic system works together with a NI Vision Builder interface. We developed a time efficient automated optical inspection process to determine the position and diameter of each micro-solder ball within a BGA array. This machine vision (MV) based setup works together with simplified image process steps for micro-solder ball position determination and diameter measurement. This approach provides a good balance between speed and accuracy. After analyzing the processed data, we represent two different position estimation methods for comparison. A dummy BGA, consists of several misaligned 300μm micro-solder balls, are assembled to a conductive substrate for testing. The test result shows that the platform can perform a continuous image acquisition of a 15fps, 640 × 480, 8-bite grayscale video.

This paper describes the measurement principle of the proposed system and its configuration, introduces the image processing, calibration, and analysis methods. The following sections of paper are platform design, image acquisition method, measurement results, and summary.

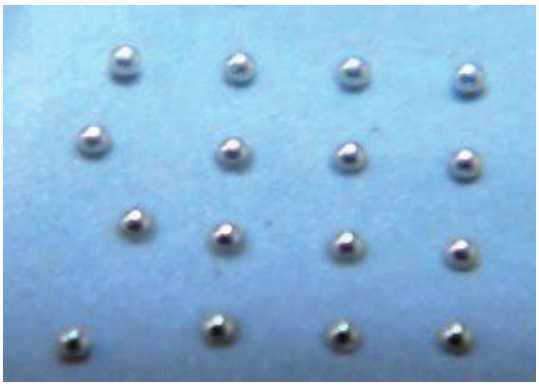

Fig. 1. Bird's-eye view photograophy of dummy ball grid array structure with misaligned balls, the diameter of the solder blalls is around 300μm. All the balls are immobilized on a conductive substrate.

978-1-4799-4726-3/14/$31.00 © 2014 IEEE

II. PLATFORM DESIGN

An experimental platform was designed and built as shown in Fig. 2. It consists of a ring light illumination unit, a macro-lens unit, an imaging unit, and an image processing and control unit.

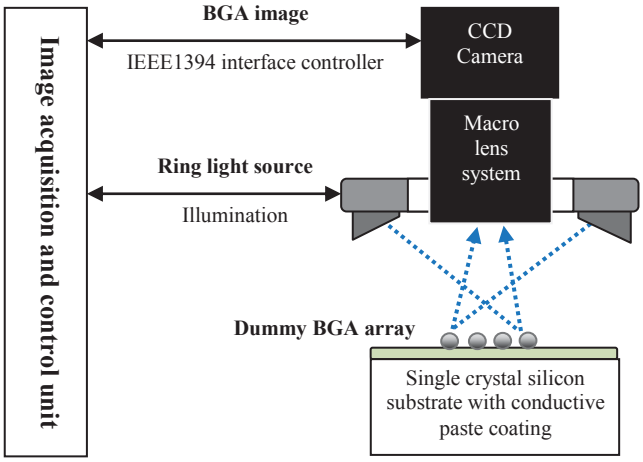

Fig. 2. Schematic of the platform setup.

The illumination unit, a white light emitting diodes (LED) ring light source, is used to eliminate shadows, which can obtain the solder ball image and project a brightest reflection spot on the top of the solder balls. Assuming the vector between the brightest reflection spot and the center of a selected solder ball is nearly perpendicular to the attached surface. It can be used to locate the ball center. The ring light source is attached to the macro-lens system above the inspection area.

The macro-lens unit is specifically installed for optimized high reproduction photography. It can achieve high magnification and long range focus, continuously from 45 mm to infinity, with broad viewing field options.

The optical imaging unit consists of a 659 × 494 pixels^2 CCD camera. Each pixel corresponds to 1.74 × 1.74μm^2 image sensing space in reality. The camera is mounted to the lens system for macro photography. The camera for image acquisition is associated with the NI-IMAQdx driver. Images are acquired from IEEE 1394 interface controller continuously under video mode (15 fps, 640 × 480, 8-bit grayscale image). This mode allows the continuous transferring and analyzing of the current image. There is no observable image aberration in this imaging unit. The photography field is adjusted to the region of interest from captured image to link and to locate the object to a pixel base coordinate system for characterization. The inspection region border should be avoided to touch any objects of interest. Corresponded to the inspection filed, video image captured from the CCD camera through the macro-lens zoom lens captured 9.3 × 9.3μm^2 square per pixel.

The image acquisition and control unit is built based on a Ni Vision Builder for automated inspection. All the image process steps are detailed in the next section.

III. IMAGE ACQUISITION METHOD

A serial image process and judgment results are detailed below. After specifying an imaging inspection area, we configure the optimized inspection I/O parameters based on experiment results.

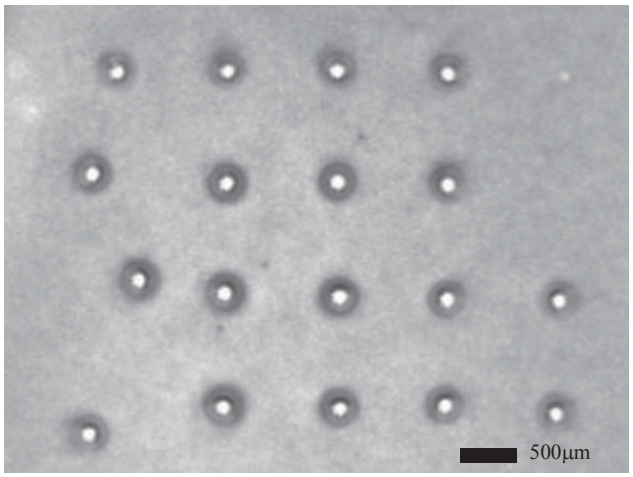

Fig. 3. Images of solder balls without shadow captured by CCD camera for image acquisition.

A. Image filtering

To remove the reflection noise of the captured image from the conductive coating, a median filter is prepared for image filtering. The nonlinear median low-pass smooth filter is assigned the median value of its eight neighborhood pixels to each pixel, which removes isolated pixels and smooth details but keeps the object contours. The size of kernel window, 8 neighborhood pixels, is obtained from experiment for the desired result.

B. Object detection, ball center estimation and area-based diameter estimation

The platform can dynamically estimate the coordinate of the targets. It continuously updates the results while Vision Builder AI runs in inspection mode. However, we use a stationary dummy BGA chip to verify the effectiveness of this platform. We set the upper threshold to isolates the pixels with intensity values between 0 and 139, to look for dark objects and to specify the type of objects. This process uses threshold and binary morphology to separate the pixels of the solder balls from background pixels.

The object detection process will crop the isolated pixels with minimized square boxes. The coordinate of the object center of the isolated pixels represents the center of each square box; it also represents the center of the solder balls, shown in Figure 4.

The detected objects are sorted by vertical position (in pixels) of the center of isolated pixels, shown in Figure 5. The detection step will return an array of numeric measurement results for analysis.

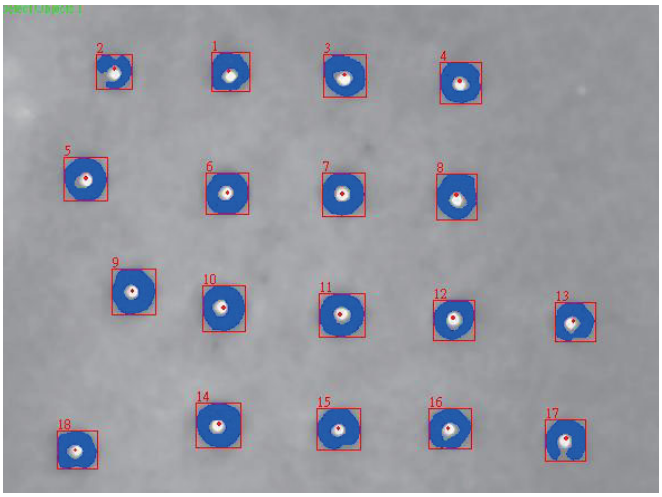

Fig. 4. Object detection and postioning: a custom overlay, includes the test numbers and squares for the cropped regions; the royal-blue patterns represent the isolated pixels of the dark objects, which grascale valuses are lower than 139.

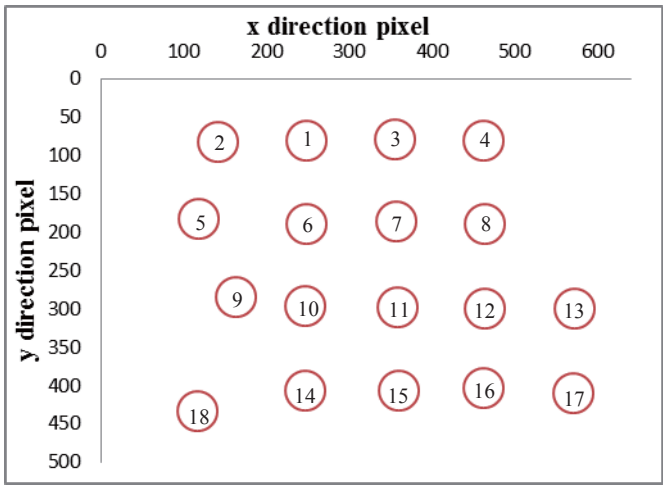

Fig. 5. Pixel coordinate and the number system of solder balls

Assuming all the solder balls are perfectly spherical and grounded to the conductive paste without any deformation. The area of each square box contains the information of diameter inspection results. One can perform simple calculation to derive the diameter of the balls from the area of the square box, as shown in follow.

From □ABCD in Fig. 6, we have：

$$\overline{AB} = \overline{AC}$$

$$Area = \overline{AB} \times \overline{AC} = {L_1}^2 \qquad (1)$$

$$\sqrt{\overline{AB} \times \overline{AC}} = 2r = d \qquad (2)$$

$$\sqrt{Area} = d \qquad (3)$$

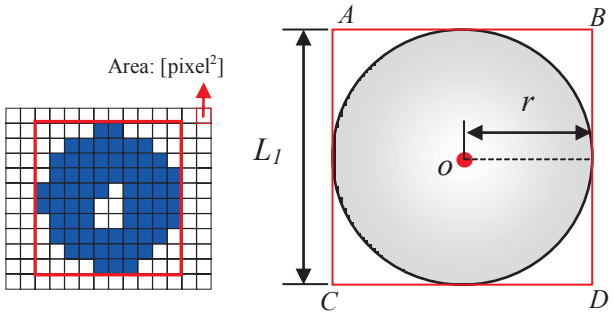

Fig. 6. Area-based diameter estimation.

C. Ball center estimation based on the brightest pixels

To determine the center of the solder balls, we take the advantages from the reflection of the ring light source on the top of the solder balls. Assuming the coordinates of the center of brightest pixel of a solder ball is matched to the coordinate location of its center. A grayscale image threshold is chosen manually based on the experiment results to isolate bright object pixels with intensity values between 253 and 255. We use the threshold-image-process to separate these brightest pixels on the tops of the balls from the background for analysis. It produces a binary image. The pixel values are set to 255 within the predetermined interval. The others are set to 0. Binary morphology can remove unwanted background. Only the pixels near the center of the ball will be taken into account, shown in Figure 7.

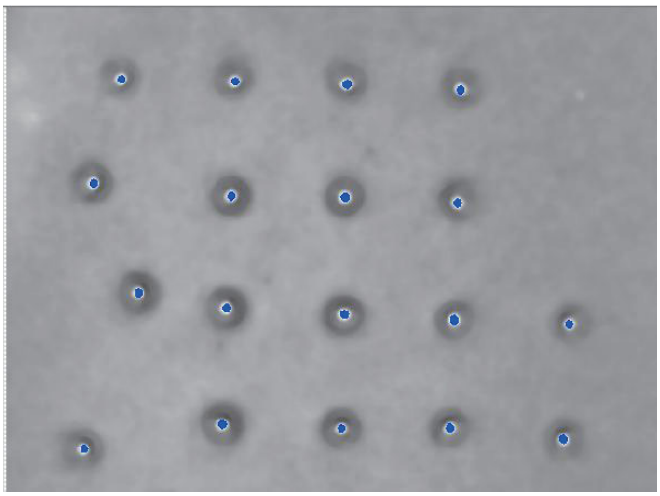

Fig. 7. Ball center postioning based on the brightest pixels; the royal-blue patterns represent the isolated pixels of the bright objects, which grascale valuses area above 253 .

When the micro solder balls are illuminated by a ring light source, reflection lights, scattering from the highest point of micro balls, are collected by the macro-lens and the camera. After similar object detection process, one can estimate the center of the solder balls. To summarize all the image acquisition steps, a flowchart is shown in Figure 8.

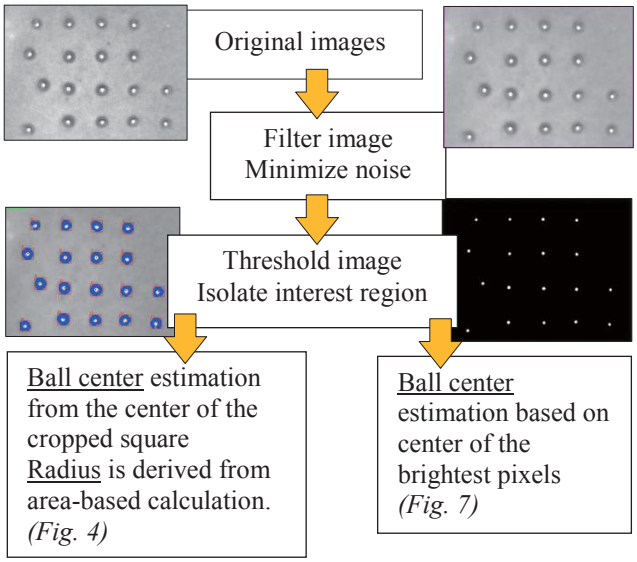

Fig. 8. Flowchart of image acquisition steps.

For a given system setup, the diameter and pixel coordinate transferring constant must be determined and calibrated prior to the inspection process. That transferring constant can be derived from a known reference length, e.g. OP-HC1, a hi-magnification calibration scale from Jingstone Corp., divided by its corresponding pixel difference. The pixel difference in the image is determined by the proposed system. Then a precision metrology reference length that overlays the measured image is fine-tuned along the perpendicular corner. Following the calibration procedure described above, the pixel difference of the metrology reference length is measured. Therefore, the value of the transferring length can be obtained (one pixel corresponded to 9.1μm). There is no double that a clear and a high-resolution image will be the key to an accurate measurement trade-off in the size of inspection field.

IV. Measurement Results

These results are also compared with the measuring from a metrology grade micro-optical scope, shown in Figure 9.

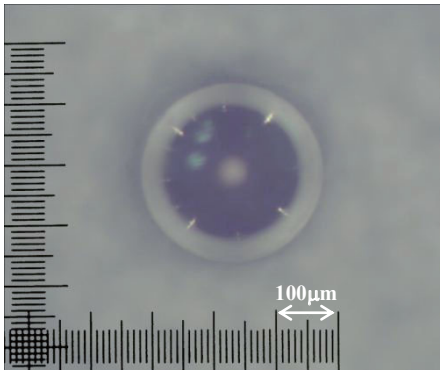

Fig. 9. Microscopic metrology photograph of a solder ball.

Table I is a list the measurement results from 18 micro-solder balls, it summarizes the diameter of each solder ball, which allows further analysis and comparisons. The diameters of the solder balls are measured from 292.0 to 322.2μm.

TABLE I. *A List the Measurement Results*

Ball #	*Microscopic metrology, measurement (μm)*	*Area-based diameter estimation (μm)*	*Ball #*	*Microscopic metrology measurement (μm)*	*Area-based diameter estimation, (μm)*
1	299.2	321.0	*10*	292.0	308.9
2	304.2	293.3	*11*	295.1	314.5
3	305.5	322.2	*12*	301.4	303.4
4	300.8	303.7	*13*	312.4	311.7
5	328.1	328.8	*14*	300.8	306.7
6	294.8	309.6	*15*	299.2	293.6
7	302.4	313.4	*16*	307.1	307.8
8	305.8	310.1	*17*	297.6	306.9
9	291.1	292.0	*18*	304.9	294.1

Targeting on a good balance between speed and accuracy, without using any computational circle fitting algorithm, e.g. [8], this approach significantly shorten the time for estimating the centers and diameters of the solder balls in a ball grid array. However, the major trade-off is the potential loss of accuracy. Table II is a list of the statistics difference between acquired image and microscopic metrology image.

TABLE II. *Comparison of Radius of Solder Balls.*

Diameter	*Microscopic metrology measurement(μm)*	*Area-based diameter estimation (μm)*
Ave. (μm)	302.9	307.1
STD(μm)	8.4	10.3
Max(μm)	328.1	328.8
Min(μm)	291.1	292.0
Ave. Difference in %	3.0%	

The statistic histogram for the measured ball diameter is shown in Fig. 10.

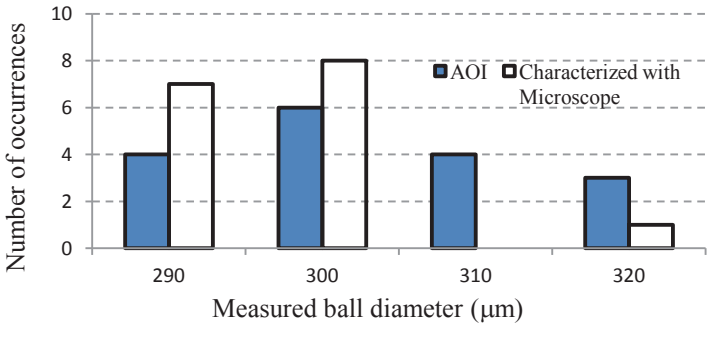

Fig. 10. The histogram displays the total number of balls for each estimated diameter value.

The histogram displays the total number of balls for each estimated diameter value. The x-axis represents the diameters of solder balls, and the y-axis represents the number of balls. The average diameter of measured results has good consistency of to the diameter judged from the metrology microscopic images; however, image filtering process may cause the redistribution of statistic histogram. The difference level is close to the half of the image pixel resolution.

Table III shows the comparison of different position measurement methods. Figure 11 shows the histogram of error distribution of different position measurement methods. The results show that the 2nd method has better accuracy than the first method.

TABLE III. ERROR COMAPSION OF DIFFERENT POSITION MEASUREMENT METHODS.

Error	*1st method : Estimated by the center of the cropped square*	*2nd method Estimated by the Brightest pixel spots on the top of the solder balls.*
Ave. Error (μm)	9.6	6.2
Max Error(μm)	44.6	22.0
Min Error(μm)	7.9	1.1

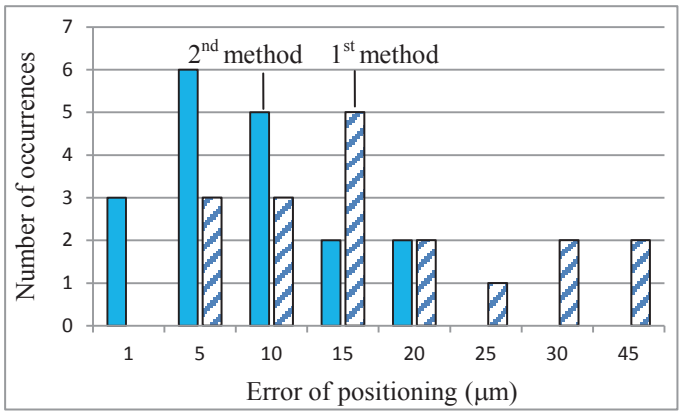

Fig. 11. Histogram of error distribution of different position measurement methods.

V. CONCLUSION

Using the proposed platform and image acquisition steps, a dummy BGA image are captured by the CCD under ring light illumination without a shadow. In order to improve the time efficiency of the automated optical inspection process, two BGA positioning methods are introduced, without using any computational circle fitting algorithm. The accuracy is mainly constrained by the image pixel resolution. The ball diameter measurement was derived from the pixel-coordinate transferring constant. The calibration of transferring constant is performed to increase the measurement accuracy. Experiments from real samples of BGA solder balls have shown that the proposed system demonstrates a good balance between image acquisition speed and accuracy. It can be easily implemented for the position inspections of BGA solder balls to estimate the yield of BGA assembly process.

VI. ACKNOWLEDGMENT

Part of this work is supported by National Science Council, NSC 100-2221-E-018-005.

REFERENCES

[1] T. Y. Tee, H. S. Ng a, D. Yap, X. Baraton, Z. Zhong, "Board level solder joint reliability modeling and testing of TFBGA packages for telecommunication applicatio," *Microelectronics Reliability.*, vol. 43, pp. 1117–1123, 2003.

[2] K. N. Tu,"Reliability challenges in 3D IC packaging technology, "*Microelectron.* Rel., vol. 51, no. 3, pp. 517–523, 2011.

[3] Y. J. Roha K. W. Ko, H. S. Choa, H. C. Kimb, H. N. Joo, S. K. Kim, "Inspection of ball grid array (BGA) solder joints using x-ray cross-sectional images," *SPIE Conf. on Machine Vision Systems for Inspection and Metrology VIII*, Boston, Massachusetts, Sep. 1999.

[4] H. N. Yen, D. M. Tsai, "A fast full-field 3D measurement system forBGA coplanarity inspection," *International Journal of AdvancedManufacturing Technology*, vol. 24, pp.132-139,2004.

[5] P. Kim, S. Rhee, "Three-dimensional inspection of ball grid arrayusing laser vision system," *IEEE Transl. on Electronics Packaging Manufacturing*, vol. 22, pp. 151-155, 1999.

[6] J. Qin,Y. Chen, F. Wang, "Solder ball height measurement by projection method,"*IEEE Transl. on Electronic Measurement & Instruments, Chengdu, China, vol. 22, pp. 101-106, 2011.*

[7] F. Wang, J. Qin, L. Han, and H. Wang, "Height measurement of micro-solder ballson metal pad by white light projection,"*IEEE Transl, Packaging and Manufacturing Technology*, vol. 2, no. 9, 2012.

[8] D. Umbach and K. N. Jones, "A Few Methods for Fitting Circles to Data," *IEEE Transactions on instrumentation and measurement,* vol. 52, no. 6, pp. 1881 -1885, December 2003.